J. Plasma Fusion Res. SERIES, Vol. 6 (2004) 581–584

Electromagnetic Effect on Turbulent Transport in Tokamak Based on Landau Fluid Global Simulation

MIYATO Naoaki[1], LI Jiquan[1,2] and KISHIMOTO Yasuaki[1]
[1]*Naka Fusion Research Establishment, JAERI, Naka, 311-0193, Japan*
[2]*Southwestern Institute of Physics, Chengdu, P. R. China*
(Received: 9 December 2003 / Accepted: 20 February 2004)

Abstract

Electromagnetic effect on ion temperature gradient driven turbulence and zonal flow generated from the turbulence is investigated based on global electromagnetic Landau fluid simulation in tokamak plasmas. Turbulent transport decreases by increasing beta in low beta regime. Two types of zonal flow are observed. One is almost stationary flow formed in low safety factor (q) region, which is weaker in higher beta. The other is flow oscillating coherently at the geodesic acoustic mode (GAM) frequency.

Keywords:

ITG turbulence, electromagnetic, finite beta, Landau fluid, zonal flow, geodesic acoustic mode

1. Introduction

It is believed that drift wave turbulence such as ion temperature gradient (ITG) driven turbulence and the zonal flow [1] generated from it are responsible for anomalous transport in tokamak plasmas. Many simulation studies for electrostatic ITG turbulence have been done based on both gyrokinetic [2] and fluid [3] models. Analytical theories for coupled system of drift wave turbulence and zonal flow also have been developed [4]. As well known the ITG instability is linearly stabilized by finite beta effect and the kinetic ballooning instability is excited above some critical beta [6], where beta is a ratio of plasma pressure to magnetic pressure. Nonlinear electromagnetic gyrofluid flux-tube simulation showed increase of transport with beta unexpected from linear estimation, whose detailed nonlinear mechanism is still unknown [5]. We have developed a global electromagnetic Landau fluid code and investigated electromagnetic effect on coupled system of microturbulence and zonal flow.

This paper is organized as follows. The numerical model is described in Sec. **2**. In Sec. **3**, results of numerical calculations are given. Finally the obtained results are summarized in Sec. **4**.

2. Model equations

We use five-field (density n, electrostatic potential ϕ, parallel component of magnetic vector potential A, parallel ion velocity v and ion temperature T) Landau fluid equation system describing the ITG mode at finite β. Compared to the previous resistive drift-Alfvén model (3-field) [7], the equation system includes an equation of parallel motion for ion fluid and an ion temperature equation with Hammett-Perkins closure [8], and an electron Landau damping model term is included in Ohm's law [5]. In the electrostatic limit with adiabatic electrons the 5-field model reduces to 3-field ion fluid model like in Refs. [9-11]. Equations for these fields are the following:

$$\frac{\mathrm{d}n}{\mathrm{d}t} = a\frac{\mathrm{d}n_{eq}}{\mathrm{d}r}\nabla_\theta\phi - n_{eq}\nabla_\parallel v + \nabla_\parallel j + \omega_d(n_{eq}\phi - \tau T_{eq}n - n_{eq}T_e) + D_n\nabla_\perp^2 n \tag{1}$$

$$\frac{\mathrm{d}}{\mathrm{d}t}\nabla_\perp^2\phi = -T_{eq}\frac{a}{n_{eq}}\frac{\mathrm{d}n_{eq}}{\mathrm{d}r}(1+\eta_i)\nabla_\theta\nabla_\perp^2\phi + \frac{1}{n_{eq}}\nabla_\parallel j - \omega_d\left(T_i + T_e + \frac{T_{eq}}{n_{eq}}(1+\tau)n\right) + D_U\nabla_\perp^4\phi \tag{2}$$

$$\frac{\mathrm{d}v}{\mathrm{d}t} = -\nabla_\parallel T - (1+\tau)\frac{T_{eq}}{n_{eq}}\nabla_\parallel n - \beta T_{eq}\frac{a}{n_{eq}}\frac{\mathrm{d}n_{eq}}{\mathrm{d}r}(1+\eta_i+\tau)\nabla_\theta A + D_v\nabla_\perp^2 v \tag{3}$$

$$\beta\frac{\partial A}{\partial t} = -\nabla_\parallel\phi + \tau\frac{T_{eq}}{n_{eq}}\nabla_\parallel n + \beta\tau T_{eq}\frac{a}{n_{eq}}\frac{\mathrm{d}n_{eq}}{\mathrm{d}r}\nabla_\theta A + \sqrt{\frac{\pi}{2}\tau\frac{m_e}{m_i}}|k_\parallel|\left(v - \frac{j}{n_{eq}}\right) - \eta j \tag{4}$$

Corresponding author's e-mail: miyaton@fusion.naka.jaeri.go.jp

©2004 by The Japan Society of Plasma Science and Nuclear Fusion Research

$$\frac{\mathrm{d}T}{\mathrm{d}t} = T_{eq}\frac{a}{n_{eq}}\frac{\mathrm{d}n_{eq}}{\mathrm{d}r}\eta_i\nabla_\theta\phi - (\Gamma-1)T_{eq}\nabla_\parallel v + T_{eq}\omega_d\left((\Gamma-1)\phi + (2\Gamma-1)T + (\Gamma-1)\frac{T_{eq}}{n_{eq}}n\right) - (\Gamma-1)\sqrt{\frac{8T_{eq}}{\pi}}|k_\parallel|T + D_T\nabla_\perp^2 T, \quad (5)$$

parallel current is related with magnetic potential through Ampère's law

$$j = -\nabla_\perp^2 A, \quad (6)$$

where, $\tau = T_{e0}/T_{i0}$, $\beta = (n_cT_c)/(B_0^2/\mu_0)$ is a half of beta value evaluated on plasma center, $\eta_i = \mathrm{d}\ln T_{eq}/\mathrm{d}\ln n_{eq}$, $n_{eq}(T_{eq})$ is an equilibrium density(ion temperature) normalized by a central value $n_c(T_c)$, B_0 is a toroidal magnetic field on a magnetic axis and $\Gamma = 5/3$ is a specific heat. We assume a circular tokamak geometry (r,θ,ζ), where r is a radius of magnetic surface, θ and ζ are poloidal and toroidal angles, respectively. Then operators are defined as

$$\frac{\mathrm{d}f}{\mathrm{d}t} = \partial_t f + [\phi, f],\ \nabla_\parallel f = \epsilon\partial_\zeta f - \beta[A, f],$$
$$\omega_d \cdot f = 2\epsilon[r\cos\theta, f],$$
$$[f, g] = \frac{1}{r}\left(\frac{\partial f}{\partial r}\frac{\partial g}{\partial\theta} - \frac{\partial f}{\partial\theta}\frac{\partial g}{\partial r}\right)$$

where $\epsilon = a/R$ is an inverse aspect ratio, a and R are minor and major radii, respectively. Here the normalizations are $tv_{ti}/a \to t$, $r/\rho_i \to r$, $\rho_i\nabla_\perp \to \nabla_\perp$, $a\nabla_\parallel \to \nabla_\parallel$,

$$\frac{a}{\rho_i}\left(\frac{n}{n_c}, \frac{e\phi}{T_c}, \frac{v}{v_{ti}}, \frac{A}{\beta B_0\rho_i}, \frac{T}{T_c}\right) \to (n, \phi, v, A, T)$$

where $v_{ti} = \sqrt{T_c/m_i}$, $\rho_i = v_{ti}/\omega_{ci}$, $\omega_{ci} = eB_0/m_i$. Artificial dissipations (D_n, D_U, D_v, D_T) are included to damp the small scale fluctuations.

3. Numerical results

Parameters used in calculations are $R/a = 4$, $\rho_i/a = 0.0125$, $\tau = 1$, $n_{eq} = 0.8 + 0.2e^{-2(r/a)^2}$, $T_{eq} = 0.35 + 0.65(1 - (r/a)^2)^2$, $q = 1.05 + 2(r/a)^2$. Nonlinear calculations have been done for $\beta = 0.001$ and 0.003. All fields are expanded in Fourier modes in the poloidal and toroidal directions,

$$f = \sum_{m,n} f_{mn}(r, t)\exp[\mathrm{i}(m\theta - n\zeta)] \quad (7)$$

and finite differenciated in the radial direction. The Fourier modes included in calculations are ones having resonant surfaces between $0.2 < r/a < 0.8$ and $(m,n) = (0,0)$, $(1,0)$ components. The number of radial mesh is 256 for $\beta = 0.001$ or 512 for $\beta = 0.003$. Since higher radial resolution is necessary for higher beta calculation, computational cost increases with beta. Analysis for higher beta will be reported in future. Artificial D's are set to be $\sim 10^{-7}\ m^4$ which is hyperviscosity-like and resistivity $\eta = 4\times10^{-5}$.

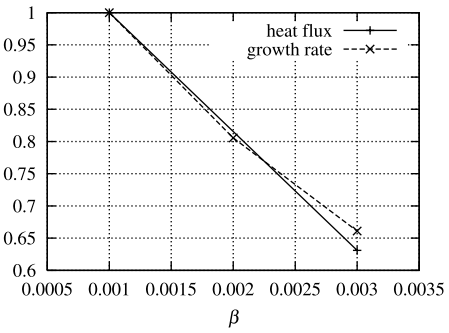

Fig. 1 Linear growth rate and mean heat flux as a function of beta. They are normalized by the value for β = 0.001

Figure 1 shows linear growth rate and heat flux as a function of beta. The ITG mode is a dominant instability in the present parameters, although kinetic ballooning mode is dominant for $\beta = 0.006$. As in Ref. [5] heat transport decreases with the linear growth rate in a low beta regime.

Figures 2 and 3 show temporal evolutions of $\boldsymbol{E}\times\boldsymbol{B}$ zonal flow and electrostatic component of heat flux $\langle\tilde{T}\tilde{v}_{Er}\rangle$ in quasi steady state for $\beta = 0.001$, respectively, where $\tilde{v}_{Er} = -\frac{1}{r}\frac{\partial\tilde{\phi}}{\partial\theta}$. Two types of zonal flow are observed in Fig. 2. In an inner (low q) region zonal flow is almost stationary. The stationary zonal flow develops around $r/a = 0.31$ and suppresses heat transport (box (a) region in Fig. 3). On the other hand, the zonal flow makes coherent oscillation due to the geodesic curvature in an outer (high q) region. The frequency of oscillation is that of geodesic acoustic mode (GAM) $\sim v_{ti}/R$. It seems that the GAM also regulates heat transport as pointed in Refs. [12,13]. When heat flux increases, subsequently zonal flow becomes strong and suppresses the heat flux (box (b) in Fig. 3 and box in Fig. 2). Time evolutions of $\boldsymbol{E}\times\boldsymbol{B}$ zonal flow for $\beta = 0.003$ are shown in Fig. 4. The stationary zonal flow around $r/a = 0.31$ is weaker than that for $\beta = 0.001$. This is due to nonlinear magnetic flutter. Maxwell stress has little effect on the zonal flow generation even in $\beta = 0.003$ case. When the magnetic nonlinear terms ($[A,]$ term in $\nabla_\parallel$) are dropped artificially, stronger zonal flow

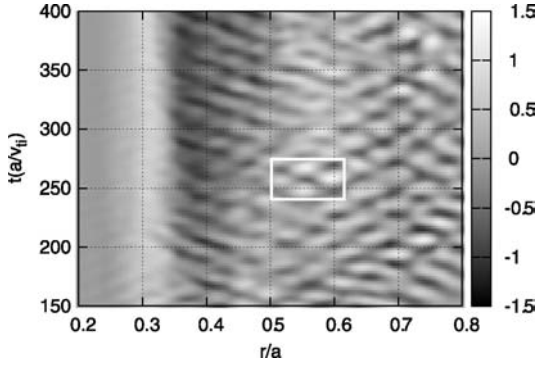

Fig. 2 Temporal evolution of $\boldsymbol{E}\times\boldsymbol{B}$ zonal flow for $\beta = 0.001$.

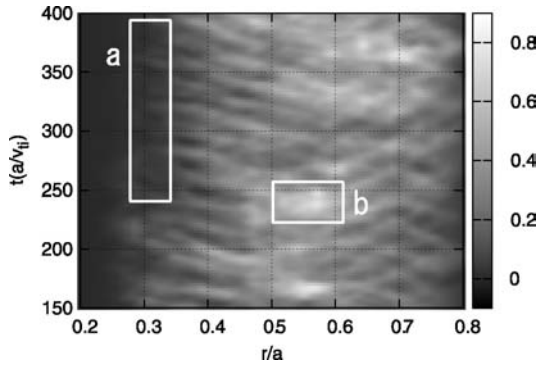

Fig. 3 Temporal evolution of heat flux for $\beta = 0.001$.

is formed like $\beta = 0.001$ case as shown in Fig. 4(nomag). There seems to be no significant change in the GAM oscillation.

Zonal flow energy equation is

$$\frac{\partial}{\partial t}\frac{1}{2}\langle v_E\rangle^2 = -\langle \tilde{v}_{Er}\tilde{\Omega}\rangle\langle v_E\rangle + \hat{\beta}\langle \tilde{B}_r\tilde{j}\rangle\langle v_E\rangle - \omega_B\langle p\sin\theta\rangle\langle v_E\rangle, \quad (8)$$

where $\langle\cdot\rangle$ denotes flux surface average, $\langle v_E\rangle = \frac{\partial\phi_0}{\partial r}$ is the $\boldsymbol{E}\times\boldsymbol{B}$ zonal flow, $\tilde{\Omega} = \nabla_\perp^2\tilde{\phi}$ is vorticity and $\omega_B = 2a/R$. The first term in the right hand side is a Reynolds stress term, the second is a Maxwell stress term and the final is a geodesic curvature term which shows the coupling with $(m,n) = (1,0)$ pressure perturbation. Here a viscous term is neglected. The average contributions to the zonal flow energy from these three terms are listed in Table 1 (the final term is labeled as GAM drive). The Reynolds stress contribution is positive and drives the zonal flow. The mean GAM drive is negative, which is a sink for the zonal flow as reported in Ref. [14]. The Maxwell stress contribution is very small compared to the other contributions, but increases with beta.

Table 1 Time averaged zonal flow energy drive due to Reynolds stress, Maxwell stress and geodesic curvature effect (GAM drive).

β	0.001	0.003
Reynolds drive	17.1	6.84
Maxwell drive	−0.182	−0.433
GAM drive	−14.7	−5.53

4. Summary

Nonlinear global simulations of electromagnetic ITG turbulence in tokamaks have been performed based on the reduced 5-field Landau fluid model and finite β effect on turbulent transport and zonal flow has been investigated in the low beta regime. The turbulent transport decreases with the linear growth rate of the ITG mode by increasing beta. Two types of zonal flow are observed. One is the almost stationary flow formed in the low q region, which is weaker at higher beta due to the nonlinear magnetic flutter. The other is the flow oscillating coherently at the GAM frequency. The Reynolds stress is a source of zonal flow energy, while the geodesic curvature related term acts as a loss channel for the zonal flow. The Maxwell stress has little effect on the zonal flow in the present parameters. But its contribution increases with beta and may be important at higher beta.

Further detailed analysis is necessary for understanding nonlinear dynamics between the ITG turbulence and the zonal flow at finite beta. And nonlinear simulations at higher beta are in underway.

References

[1] A. Hasegawa and M. Wakatani, Phys. Rev. Lett. **59**, 1581 (1987).
[2] Z. Lin *et al.*, Phys. Rev. Lett. **83**, 3645 (1999).
[3] I. Voitsekhovitch *et al.*, Phys. Plasmas **9**, 4671 (2002).
[4] P.H. Diamond *et al.*, Nucl. Fusion **41**, 1067 (2001).
[5] P.B. Snyder and G.W. Hammett, Phys. Plasmas **8**, 744 (2001).
[6] J.Y. Kim *et al.*, Phys. Fluid B **5**, 4030 (1993).
[7] N. Miyato, S. Hamaguchi and M. Wakatani, Plasma Phys. Control. Fusion **44**, 1689 (2002).

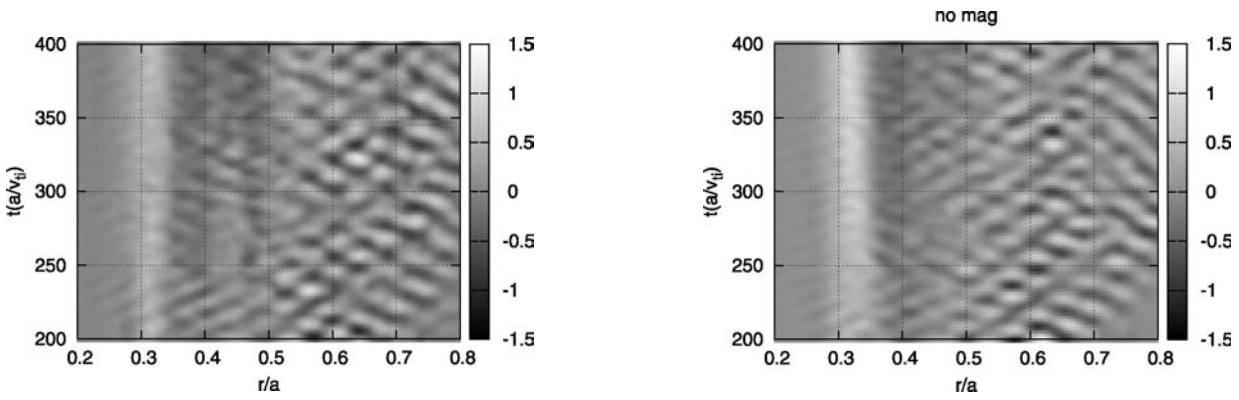

Fig. 4 Temporal evolutions of $\boldsymbol{E}\times\boldsymbol{B}$ zonal flow for $\beta = 0.003$. The figure labeled "nomag" shows the zonal flow in the case without magnetic nonlinearity.

[8] G.W. Hammett and F.W. Perkins, Phys. Rev. Lett. **64**, 3019 (1990).
[9] N. Mattor, Phys. Fluid B **4**, 3952 (1992).
[10] J.N. Leboeuf *et al.*, Phys. Plasmas **7**, 5013 (2000).
[11] X. Garbet *et al.*, Phys. Plasmas **8**, 2793 (2001).
[12] K. Hallatschek and D. Biskamp, Phys. Rev. Lett. **86**, 1223 (2001).
[13] M. Ramisch *et al.*, New J. Phys. **5**, 12.1 (2003).
[14] B. Scott, Phys. Lett. A **320**, 53 (2003).